FACTA UNIVERSITATIS
Series: **Physics, Chemistry and Technology** Vol. 20, Nº 1, 2022, pp. 55 - 65
https://doi.org/10.2298/FUPCT2201055S

Original scientific paper

SHAPING THE DYNAMICS OF AHARONOV-BOHM CAGED LOCALIZED MODES BY NONLINEARITY

UDC 537.533:535.513:539.124

Miljana G. Stojanović[1], Ana Mančić[2], Milutin Stepić[1], Aleksandra Maluckov[1]

[1]COHERENCE, Department of Atomic Physics, Vinča Institute of Nuclear Sciences, National Institute of Republic of Serbia, University of Belgrade, Belgrade, Serbia
[2]COHERENCE, Department of Physics, Faculty of Sciences and Mathematics, Niš, Serbia

Abstract. *Two-dimensional dice lattice can be dressed by artificial flux to host the Aharonov-Bohm (AB) caging effect resulting in the occurrence of a fully flatband spectrum. Here, we focus on the dynamics of flatband compact localized eigenmodes shared by a few unit cells in two snowflake configurations. We numerically show the possibility of dynamically stable propagation of two types of compact localized complexes by tuning the nonlinearity. The AB caging is imprinted in complexes dynamics regardless of the type and strength of nonlinearity. On the other hand, nonlinearity can only affect the appearance of the caged complex. These findings open a new route for the manipulation of structured light in photonic systems.*

Key words: *lattice, Aharonov-Bohm caging, flatband spectrum, compacton, nonlinearity*

1. INTRODUCTION

Flatband (FB) photonic lattices have been captivating the attention of investigators in photonics by offering an easy, manageable platform for testing the possibilities to slow, trap and manipulate light propagation by mimicking the basic algebraic, logical operations and providing the efficient information storage (Leykam et al., 2018, Morales-Inostroza et al., 2016, Zhang and Jin, 2020, He et al. 2021, Vicencio, 2021). Regarding this, playing with individual photons is, nowadays, the leading and promising experimental procedure toward the realization of efficient quantum computing with the potential to jump over the limitations of procedures based on spin/atomic systems (Leykam and Flach, 2018). Moreover, the

Received: January, 31st, 2022; accepted: July, 5th, 2022
Corresponding author: Mirjana Stojanović, Department of Atomic Physics, Vinča Institute of Nuclear Sciences, National Institute of Republic of Serbia, University of Belgrade, P.O. Box 522, 11001 Belgrade, Serbia; e-mail: mirjana.stojanovic@vin.bg.ac.rs

manipulation of photon lattice geometry and topology provides the test bed for understanding the topological phase transitions in condensed matter systems (Lisi et al., 2021, Derzhko et al., 2015, Aoki, 2020, Yang et al., 2015, Aharonov and Bohm, 1959).

The main property of the FB systems is the absence of dispersion which opens the door to an amazing world of fully degenerate energy bands and offers the possibility for tailoring the light/photon properties by forming compactons – isolated localized structures highly robust to environmental noise. Due to their easy manipulation, photonic lattices are an ideal platform for creating FB spectrums. Their geometry provides the possibility to design artificial gage field effects equivalent to the magnetic field flux, i.e. the spin-orbit interaction in atomic systems (Lisi, et al., 2021, Jörg, et al., 2020, Parameswaran et al. 2013). A few experimental techniques providing this in practice are based on the coupled split-ring resonators (Leykam and Yuan, 2020, Liang and Chong, 2013, Leykam et al., 2017, Mittal et al., 2016) and wave-guide networks (Morales-Inostroza et al., 2016, Mukherjee et al., 2016, Real, et al., 2017, Vicencio et al., 2015) Peculiar in the flatband world are systems with a fully flat spectrum which are usually related to the effect of the Aharonov-Bohm (AB) caging (Mukherjee et al., 2016, Vidal, J. et al., 2001, Danieli et al., 2021, Vidal et al., 1998). The study of AB effects in photonic lattices dates from the paper of Longhi (Longhi, 2014) and is widely exploited in 1D and 2D photonic lattice systems (Danieli et al., 2021, Verboven, 2016). We mention the lattice shaking as a mechanism for constructing a net flux through a plaquette which is equivalent to adding a time-periodic on-site modulation term to Hamiltonian (Floquet lattices) (Creffield et al., 2016). Recently, the FB system is probed by nonlinearity in order to find new possibilities to control light of huge intensity (Gligorić et al., 2019).

In this paper, we study an interesting aspect of the compact localized modes (CLMs) in two-dimensional (2D) dice lattices dressed by artificial flux. This lattice can host six FBs (Zhang and Jin, 2020) in the presence of local nonlinearity. The model equations and linear lattice spectrum properties are described in Section 2. We test the dynamics of the snowflake-like CLMs hosted by a few unit cells in the linear and nonlinear regimes in Section 3. The goal is to confront the AB caging to nonlinearity in order to distinguish the favorable conditions for designing the localized modes with user-friendly properties. Concluding remarks are given in Section 4.

2. MODEL

The dice lattice is a paradigm of the 2D flux-dressed photonic lattices which mimic the topological phases in atomic systems (Vidal et al., 2001, Danieli et al., 2021, Vidal et al., 1998, Zhang and Jin, 2020, Verboven, 2016). Its geometry is schematically shown in Fig. 1 and it can be constructed by overlapping two hexagonal lattices in the flux-free case. In the presence of gauge field-induced artificial magnetic flux, the unit cell can be identified as a structure consisting of six sites, denoted by a, b, c, d, e, and f, which are linearly coupled by complex hopping $te^{i(\phi/2)}$, as shown in Fig. 1, where t is the hopping parameter and the ϕ is artificial flux.

Sites c and d are 6-fold coordinated (hub-sublattices) and sites a, b, e, and f are 3-fold coordinated (rim-sublattices). Each diamond plaquette, which is the building block of the

dice lattice encloses a half-quantum artificial magnetic flux π or –π (yellow and green diamonds in Fig. 1, respectively).

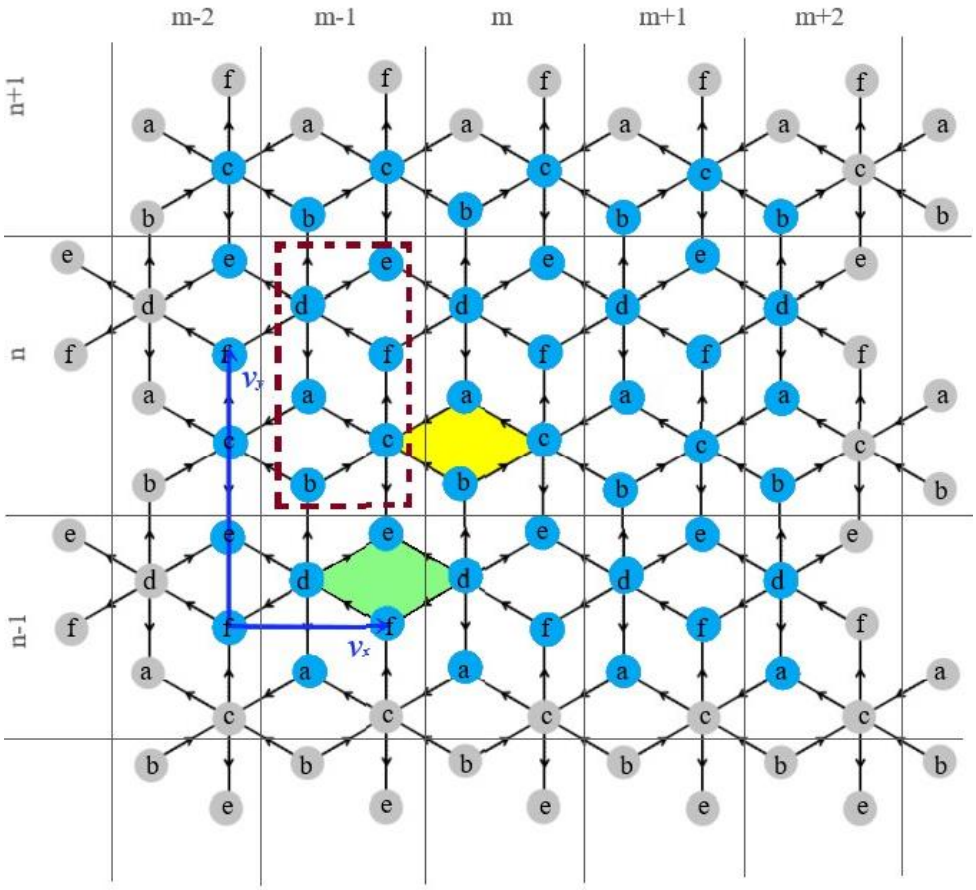

Fig. 1 Schematic representation of the 2D dice lattice. The unit cell of the dice lattice is denoted by a dashed rectangle. The sites are denoted with a, b, c, d, e, and f and n, m are the cell indices. The vectors $\mathbf{v}_x$ and $\mathbf{v}_y$ in the horizontal and vertical directions are indicated by the dark blue arrows. The two types of diamond plaquettes are shaded in yellow and green.

The light propagation through the nonlinear flux-dressed dice lattice in the tight-binding approximation can be modeled by a set of 6MN coupled differential equations with the on-site cubic nonlinear terms:

$$\begin{aligned}
i\dot{a}_{m,m} + t(c_{m,n} + d_{m,n})e^{-i\frac{\phi}{2}} + tc_{m-1,n}e^{i\frac{\phi}{2}} + \gamma \mid a_{m,n} \mid^2 a_{m,n} = 0,\\
i\dot{b}_{m,n} + t(c_{m,n} + c_{m-1,n})e^{i\frac{\phi}{2}} + td_{m,n-1}e^{-i\frac{\phi}{2}} + \gamma \mid b_{m,n} \mid^2 b_{m,n} = 0,\\
i\dot{c}_{m,n} + t(a_{m,n} + f_{m,n} + e_{m,n-1})e^{i\frac{\phi}{2}} + t(b_{m,n} + a_{m+1,n} + b_{m+1,n})e^{-i\frac{\phi}{2}} + \gamma \mid c_{m,n} \mid^2 c_{m,n} = 0,\\
i\dot{d}_{m,n} + t(a_{m,n} + e_{m,n} + e_{m-1,n} + f_{m-1,n} + b_{m,n+1})e^{i\frac{\phi}{2}} + tf_{m,n}e^{-i\frac{\phi}{2}} + \gamma \mid f_{m,n} \mid^2 f_{m,n} = 0,\\
i\dot{e}_{m,n} + t(d_{m,n} + d_{m+1,n} + c_{m,n+1})e^{-i\frac{\phi}{2}} + \gamma \mid e_{m,n} \mid^2 e_{m,n} = 0,\\
i\dot{f}_{m,n} + td_{m,n}e^{i\frac{\phi}{2}} + t(c_{m,n} + d_{m+1,n})e^{-i\frac{\phi}{2}} + \gamma \mid f_{m,n} \mid^2 f_{m,n} = 0.
\end{aligned} \tag{1}$$

where dot signs the derivation with respect to the propagation coordinate z, NM is the total number of cells and the composite complex wave function is represented by the 6 - component spinor in each cell $(abcdef)^T_{m,n}$ (m, n are the cell indices). The strength of the complex hopping parameter is scaled to $t = 1$ in the following, and γ is the nonlinear coefficient.

The Hamiltonian in the reciprocal lattice space is obtained by applying the 2D Fourier transformations regarding the translation invariance of the 2D periodic dice lattice in both horizontal and vertical directions (Zhang and Jin, 2020):

$$H = t\begin{bmatrix}
0 & 0 & f_1 & f_2 & 0 & 0\\
0 & 0 & f_3 & f_4^* f_2 & 0 & 0\\
f_1^* & f_3^* & 0 & 0 & f_4^* f_2^* & f_2^*\\
f_2^* & f_2^* f_4 & 0 & 0 & f_3 & f_1\\
0 & 0 & f_4 f_2 & f_3^* & 0 & 0\\
0 & 0 & f_2 & f_1^* & 0 & 0
\end{bmatrix} \tag{2}$$

where $f_1 = e^{-i\frac{\phi}{2}} + e^{i\frac{\phi}{2}}e^{-ik_x}$, $f_2 = e^{-i\frac{\phi}{2}}$, $f3 = (1 + e^{-ik_x})e^{i\frac{\phi}{2}}$, $f_4 = e^{ik_y}$.

The six eigenenergies of linear Hamiltonian form four dispersive bands and one doubly degenerated FB for $\phi = 0$, as shown in Fig. 2a. Changing the value of flux, a set of three momentum independent, fully degenerated FBs is obtained for $\phi = \pi$, Fig. 2b. Corresponding eigenvectors form the Bloch wave basis, which can be expressed in a form $\psi_{m,n} = \psi_{m,n}e^{-i(k_x m + k_y n)}e^{-i\beta z}$, where β is the corresponding eigenenergy value which plays a role of propagation constant, and k_x, k_y are components of the transversal 2D wave vector ***k***.

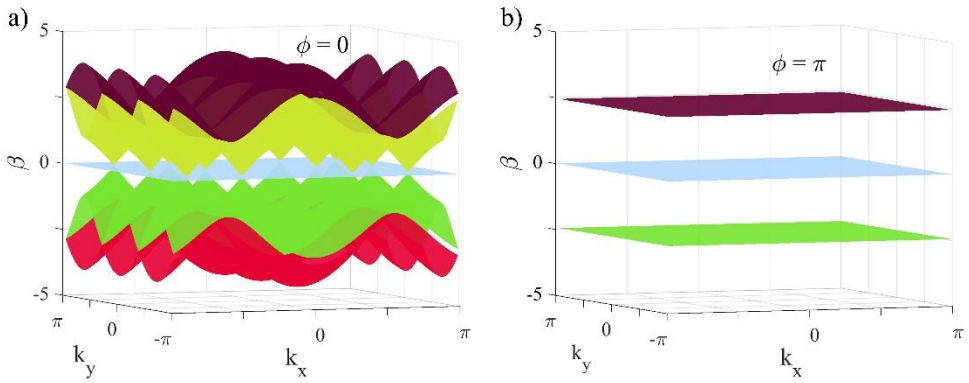

Fig. 2 The energy band spectrum of linear dice lattice for two values of flux: a) $\phi = 0$ and b) $\phi = \pi$.

In the fully FB case, $\phi = \pm\pi$ a set of CLMs, i. e. compactons, can be obtained as a result of the superposition of Bloch states under conditions of destructive interference. They are hosted by a few unit cells in the form of six snowflake-like localized structures, Fig. 3 [7].

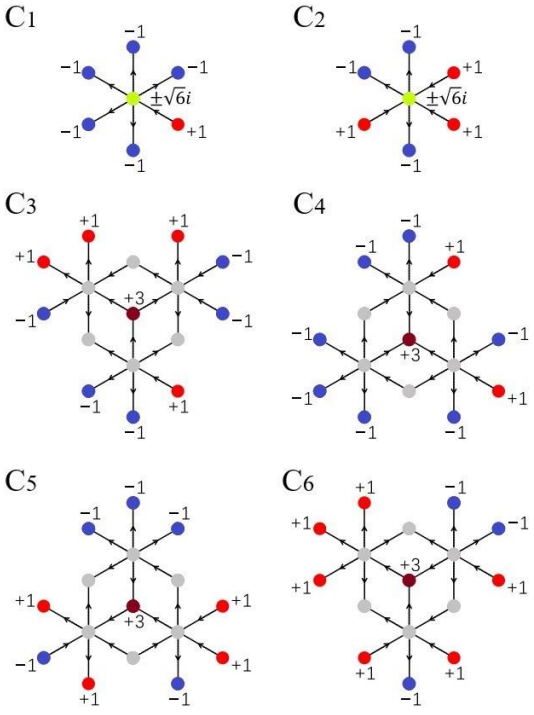

Fig. 3 Schematic representation of the six types of CLMs of the dice lattice. The energies of the CLMs are $\pm\sqrt{6}$ for the top panel and 0 for the middle and bottom panels. The C_1 and C_2 are centered at hub-sublattices, while C_3-C_6 are centered at rim-sublattices. The nonzero values of amplitude are written in corresponding plots.

The fundamental compactons of $C_{1,2}$ type, belonging to non-zero FBs, are hosted by 3 unit cells, while quartet $C_{3\text{-}6}$, belonging to zero energy FB, is hosted by 6 unit cells. By translating the fundamental compactons, the compact but not orthogonal eigenbasis can be defined. The properties of the FB compactons are investigated in the dice lattice in detail (Zhang and Jin, 2020). Here, we clarify the dynamics of these modes in linear as well as nonlinear dice lattices.

We propagate the CLMs through the dice lattice by numerically solving the model Eq. 1. The results illustrated in the following are obtained for the dice lattice with 15x15 unit cells. The environmental noise is modeled as uniform random events, i. e. as white noise (Stojanović et al., 2021), and propagation is simulated by adopting the Runge-Kutta procedure of the 6^{th} order. In order to scan the dynamical properties of the CLMs, we calculate the participation number *Pn*, which is proportional to the number of sites on which the mode is localized; mode overlapping ρ, which represents the normalized magnitude of field overlap; and total intensity distribution *I*. The evolution of these quantities shows the efficiency of the mode compactness-localization and offers a possibility of estimating which mechanism governs the mode dynamics.

3. COMPACT LOCALIZED MODE DYNAMICS

3.1. Linear case

Regarding the linear propagation of CLMs modes under the fulfilled conditions for AB caging, the dynamical properties are fully determined by the non-orthogonality i.e. linear dependence of the CLMs spanning the same energy band. We have found two types of dynamically steady compact structures. The first one is formed by C_1, C_5, and C_6, which keeps initial snowflake-like structures hosted by 3 (C_1) and 6 cells (C_5, and C_6,) during the propagation, as shown in Fig. 3. We can notice the small amplitude oscillations (Fig. 4a) in the *Pn* and ρ values during the whole propagation with period Z_0=2.5. In addition, the intensity distribution stays mostly frozen, hence indicating stable mode propagation.

The second peculiar dynamical structure is a breather which is formed by the propagation of the C_2, C_3, and C_4. In Fig. 4b the Pn and ρ vs. z oscillate with two characteristic periods, Z_0 and Z_1, with Z_1/Z_0=1/2, directly related to the AB caging which traps C_2 dynamics to 6 and $C_{3,4}$ to 12 cells. The intensity distribution dynamics fully correlate with the participation number and mode overlapping behavior as illustrated in Fig. 5 for the C_3 mode initially injected in the lattice. In this figure, four different time snapshots of the total intensity of the resulting breather over one period are shown representing direct proof of the efficiency of the AB caging.

We propose that the initial phase distribution among the excited CLM sites and related symmetry properties are responsible for different CLM dynamics presented above: the C_1, C_5, and C_6 stay mostly fully trapped in the initially excited sites, while C_2, C_3, and C_4 wander between the whole trapping region consisting of 6 and 12 cells, respectively.

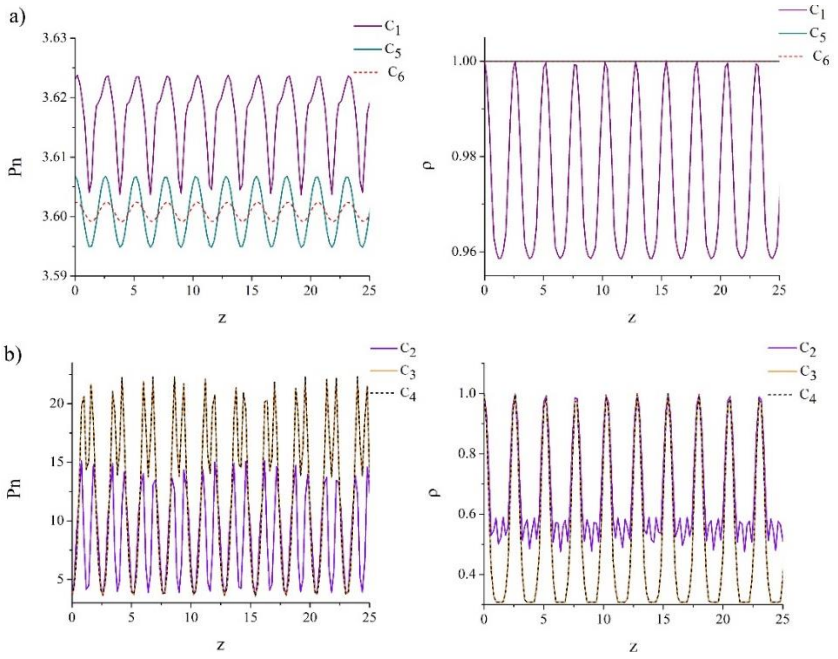

Fig. 4 The participation number (Pn) and mode overlapping (ρ) vs. propagation length (z) for each of FB compactons injected in the linear dice lattice with 15x15 unit cells.

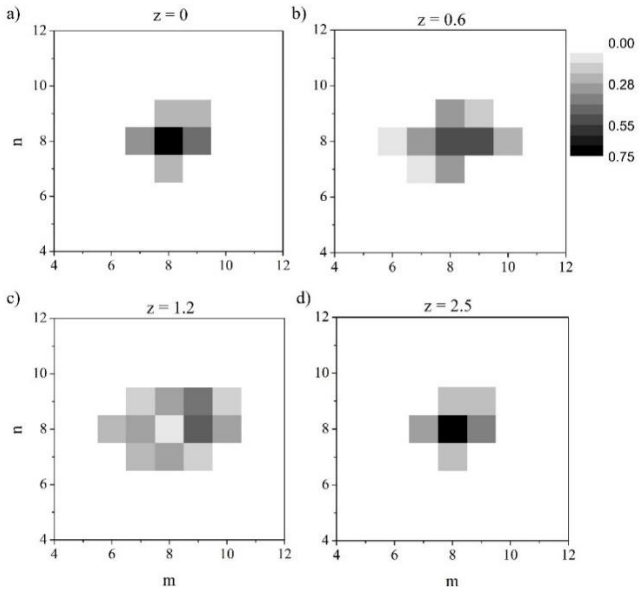

Fig. 5 The total intensity distribution of the C_3 initially injected in dice lattice at certain time instants (values of z written on plots in arbitrary units). The oscillatory dynamics inside the AB cage indicated in Figure 4 are illustrated. Mode dynamics are trapped in 12 unit cells.

3.2. Nonlinear case

Except for being non-orthogonal, the FB compact modes are heterogeneous structures. Therefore, the on-site nonlinearity cannot extend to the nonlinear CLMs' families with the same amplitude and phase distribution (Danieli et al., 2018) as was the case for homogenous compactons. However, the AB caging ensures they evolve in dynamical complexes which stay trapped inside the cage.

To probe the CLMs' robustness in the presence of nonlinearity, we propagate the snowflake-like compact modes through the lattices whose index of refraction is modified by nonlinearity. Mathematically, it is modeled by the on-site nonlinear terms in each of the system equations (Eq. 1).

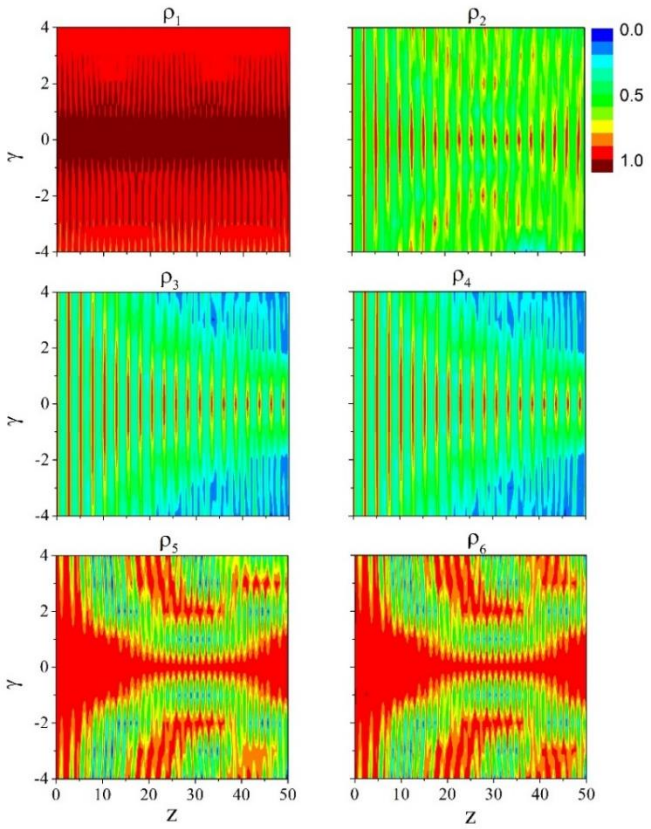

Fig. 6 The evolution of the mode overlapping vs. the nonlinearity strength for six types of compact snowflake structures in a nonlinear lattice. The high robustness of C_1, C_5, and C_6 regardless of the nonlinearity strength is obvious and can be related to the initial CLMs phase distribution (see Section 2).

For weak nonlinearity of both signs (self-focusing and self-defocusing), the nonlinear CLMs dynamics follow the patterns observed in the cases with the linear counterparts. This can be seen in Fig. 6 which presents the contour plots of the ρ(z) vs. γ. Subplots correspond

to different types of initially injected snowflake compact modes. The CLMs structures C_1, C_5, and C_6, whose extreme robustness was indicated in the linear regime, propagate without qualitative changes in the presence of weak nonlinearity, while, by increasing the strength of nonlinearity, we observe the characteristic breathing patterns with two main periods in the later propagation stages.

The CLM of a breather type keeps its main properties as well, showing the breathing pattern for weak γ with the same periodicity as in the linear case. On the other hand, the strong nonlinearity succeeds in breaking the characteristic snowflakes energy redistribution after a certain propagation length, causing the quasi-periodic breather behavior which stays caged. This confirms the significance of the AB caging despite the nonlinearity strength. In Fig. 7 the power spectrum of the quasi-periodic breather is shown and it is compared with one of the regular breathers. The increased breather complexity is associated with the widening of the spectrum lines at characteristic frequencies.

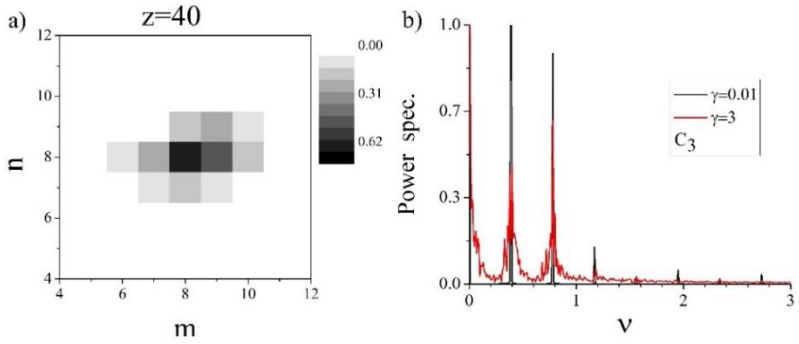

Fig. 7 a) Stroboscopic plot of the total intensity at z=40. Initially, C_3 is injected in the nonlinear lattice, γ=3. The second plot b) comparatively shows the power spectrum of the same mode in the presence of weak nonlinearity γ =0.01 and when γ =3.

4. CONCLUSIONS

The linear 2D dice lattice's energy spectrum can be tuned by an effective magnetic flux to provide the conditions for AB caging, giving rise to a fully FB spectrum. It consists of three double degenerated bands which can be spanned over the 2D wave-vectors space by compact but not-orthogonal basis of CLMs in six different snowflakes' configurations. These heterogeneous isolated localized structures owe their existence to destructive interference hosted by a few unit cells. We have been studying the dynamics of CLM in linear and nonlinear lattice environments by adopting direct numerical simulations based on the Runge-Kutta procedure. Two types of dynamical compact localized patterns have been found: highly robust snowflake-like steady compact modes in both linear and weak nonlinear lattice, and localized breather complexes robust to the presence of weak nonlinearity. The robustness of the dynamically compact modes is a consequence of the AB caging prevalence in the mentioned circumstances. The signatures of the AB caging have not been lost by increasing the nonlinearity strength, although the complexity of caged breathing modes was increased. The influence of nonlinearity can be connected with the appearance of quasi-periodic and irregular breathing structures. To conclude, we have shown the high efficiency of the AB caging in the

nonlinear 2D photonic dice lattice which offers a tool for managing and manipulating the compact localized mode dynamics. This can be tested on photonic platforms such as the arrays of ring resonators or waveguide networks in the laboratory and it can have diverse practical applications.

Acknowledgement: *This research was supported by the Ministry of Education, Science and Technological Development of the Republic of Serbia (451-03-9/2021-14/ 200017 and 451-03-9/2021-14/200124).*

REFERENCES

Aharonov Y., Bohm, D., 1959. Phys. Rev., 115(3), 485, doi:10.1103/PhysRev.115.485
Aoki, H., 2020. J. Supercond. Nov. Magn., 33, 1557-1947, doi:10.1007/s10948-019-05366-4
Creffield, C. E., Pieplow, G., Sols, F., Goldman, N., 2016. New J. Phys., 18, 093013, doi:10.1088/1367-2630/18/9/093013
Danieli, C., Andreanov, A., Mithun, T., Flach, S., 2021. Phys. Rev. B, 104(8), 085131, doi:10.1103/PhysRevB.104.085131
Danieli, C., Maluckov, A., Flach, S., 2018. Low Temp. Phys., 44, 678-687, doi:10.1063/1.5041434
Derzhko, O., Richter, J., Maksymenko, M., 2015. Int. J. Mod. Phys. B, 29,
1530007, doi:10.1142/S0217979215300078
Gligorić, G., Beličev, P. P., Leykam, D., Maluckov, A., 2019. Phys. Rev. A, 99, 013826, doi:10.1103/PhysRevA.99.013826
Gligorić, G., Leykam, D., Maluckov, A., 2020. Phys. Rev. A, 101, 023839, doi:10.1103/PhysRevA.101.023839
He, Y., Mao, R., Cai, H., Zhang, J. X., Li, Y., Yuan, L., Zhu, S.J., Wang, D. W., 2021. Phys. Rev. Lett., 126, 103601, doi:10.1103/PhysRevLett.126.103601
Jörg, C., Queraltó, G., Kremer, M., Pelegrí, G., Schulz, J., Szameit, A., Freymann, G., Mompart, J., Ahufinger, V., 2020. Light: Science & Applications, 9, 1-7, doi:10.1038/s41377-020-00385-6
Leykam, D., Andreanov, A., Flach, S., 2018. Adv. Phys. X, 3, 1473052, doi:10.1080/23746149.2018.1473052
Leykam, D., Bliokh, K. Y., Huang, C., Chong, Y. D., Nori, F., 2017. Phys. Rev. Lett., 118, 040401, doi:10.1103/PhysRevLett.118.040401
Leykam, D., Flach, S., 2018. APL Photonics, 3, 070901, doi:10.1063/1.5034365
Leykam, D., Yuan, L., 2020. Nanophotonics, 9, 4473-4487, doi:10.1515/nanoph-2020-0415
Liang, G. Q., Chong, Y. D., 2013. Phys. Rev. Lett., 110, 203904, doi:10.1103/PhysRevLett.110.203904
Lisi, S., Lu, X., Benschop, T., de Jong, T. A., Stepanov, P., Duran, J. R., Margot, F., Cucchi, I., Cappelli, E., Hunter, A., Tamai, A., Kandyba, V., Giampietri, A., Barinov, A., Jobst, J., Stalman, V., Leeuwenhoek, M., Watanabe, K., Taniguchi, T., 2021. Nat. Phys., 17, 189–193, doi:10.1038/s41567-020-01041-x
Longhi, S., 2014. Opt. Lett., 39, 5892, doi:10.1364/OL.39.005892
Mittal, S., Ganeshan, S., Fan, J., Vaezi, A., Hafezi, M., 2016. Nat. Photonics, 10, 180-183, doi:10.1038/nphoton.2016.10
Morales-Inostroza, L., Vicencio, R. A., 2016. Phys. Rev. A, 94, 043831, doi:10.1103/PhysRevA.94.043831
Mukherjee, S. Di Liberto, M., Öhberg, P., Thomson, R. R., Goldman, N., 2018. Phys. Rev. Lett.,121, 075502, doi: 10.1103/PhysRevLett.121.075502
Mukherjee S., Thomson, R. R., 2017. Opt. Lett., 42, 2243-2246, doi:10.1364/OL.42.002243
Parameswaran, S. A., Roy, R., Sondhi, S. L, 2013. CR Phys., 14, 816-839, doi:10.1016/j.crhy.2013.04.003
Real, B., Cantillano, C., López-González, D., Szameit, A., Aono, M., Naruse, M., Kim, S. J., Wang, K., Vicencio, R. A., 2017. Sci. Rep., 7, 15085, doi:10.1038/s41598-017-15441-2
Stojanović, M. G., Gündoğdu, S., Leykam, D., Angelakis, D. G., Stojanović-Krasić, M., Stepić, M., and Maluckov, A., 2021. arXiv preprint arXiv:2111.13387
Verboven, T., 2016. Master Thesis: Generating Gauge Fields in Optical Kagome and Dice Lattices. Institute for Theoretical Physics, Utrecht; Institute of Photonic Sciences, Barcelona.
Vicencio, R. A., 2021. Adv. Phys. X, 6:1, doi:10.1080/23746149.2021.1878057
Vicencio, R. A., Cantillano, C., Morales-Inostroza, L., Real, B., Mejía-Cortés, C., Weimann, S., Szameit, A., Molina, M. I., 2015. Phys. Rev. Lett., 114, 245503, doi:10.1103/PhysRevLett.114.245503
Vidal, J., Butaud, P., Douçot, B., Mosseri, R., 2001. Phys. Rev. B, 64, 155306, doi:10.1103/PhysRevB.64.155306
Vidal, J., Mosseri, R., Douçot, B., 1998. Phys. Rev. Lett., 81, 5888, doi:10.1103/PhysRevLett.81.5888

Yang, Z. H., Wang, Y. P., Xue, Z. Y., Yang, W. L., Hu, Y., Gao, J. H., Wu, Y., 2016. Phys. Rev. A, 93, 062319, doi:10.1103/PhysRevA.93.062319
Zhang, S. M., Jin, L., 2020. Phys. Rev. B 102, 054301, doi:10.1103/PhysRevB.102.054301

OBLIKOVANJE DINAMIKE AHARONOV-BOHM ZAROBLJENIH LOKALIZOVANIH MODA POSREDSTVOM NELINEARNOSTI

Uslovi za generisanje Aharonov-Bohm (AB) efekta mogu se postići u dvodimenzionalnoj rombičnoj rešetki s veštački indukovanim fluksom, što dovodi do formiranja energetskog spektra s potpuno ravnim zonama. U radu, akcenat je stavljen na proučavanje dinamike kompaktnih lokalizovanih svojstvenih moda ravnih zona, koje su izolovane na svega nekoliko jediničnih ćelija rešetke u dve pahuljičaste konfiguracije. Numerički je pokazana mogućnost stabilnog prostiranja dva tipa kompaktnih lokalizovanih kompleksa uz pogodno podešavanje nelinearnih svojstava rešetke. AB zarobljavanje igra dominantnu ulogu kada je reč o dinamici kompleksa, bez obzira na vrstu i jačinu nelinearnosti, koja, sa svoje strane, može uticati na oblik zarobljene strukture. Naša otkrića pružaju nove mogućnosti za unapređivanje načina za manipulisanje svetlošću u fotonskim sistemima.

Ključne reči: *rešetka, Aharonov-Bom kavez, energetski spektri sa ravnim zonama, kompakton, nelinearnost*